Received: 26 December 2017 | Accepted: 23 May 2018

DOI: 10.1002/hyp.13172

RESEARCH ARTICLE

WILEY

Spatial and temporal variability of 0- to 5-m soil–water storage at the watershed scale

Zihuan Fu[1,2] | Yunqiang Wang[1,3] | Zhisheng An[1,3] | Wei Hu[4] | Khan M.G. Mostofa[2] | Xuezhang Li[5] | Bingxia Liu[6]

[1] State Key Laboratory of Loess and Quaternary Geology, Institute of Earth Environment, Chinese Academy of Sciences, Xi'an 710061, China

[2] Institute of the Surface-Earth System Science Research, Tianjin University, Tianjin 300072, China

[3] Interdisciplinary Research Center of Earth Science Frontier, Beijing Normal University, Beijing 100875, China

[4] The New Zealand Institute for Plant & Food Research Limited, Private Bag 4704, Christchurch 8140, New Zealand

[5] Institute of Subtropical Agriculture, Chinese Academy of Sciences, Key Laboratory for Agro-ecological Processes in Subtropical Region, Changsha 410125, China

[6] Institute of Genetics and Developmental Biology, Chinese Academy of Sciences, Key Laboratory of Agricultural Water Resources, Center for Agricultural Resources Research, Shijiazhuang 050021, China

Correspondence
Yunqiang Wang, State Key Laboratory of Loess and Quaternary Geology, Institute of Earth Environment, Chinese Academy of Sciences, Xi'an 710061, China.
Email: wangyq@ieecas.cn

Funding information
The Coordination Innovation Project on Shaanxi Province Science and Technology, Grant/Award Number: 2015KTZDNY01-04; The National Natural Science Foundation of China, Grant/Award Numbers: 41571130083, 41530854 and 41471189; Youth Innovation Promotion Association CAS

Abstract

Dynamic relationships among rainfall patterns, soil water distribution, and plant growth are crucial for sustainable conservation of soil and water resources in water-limited ecosystems. Spatial and temporal variation in deep soil water content at a watershed scale have not yet been characterized adequately due to the lack of deep soil water data. Deep soil–water storage (SWS) up to a depth of 5 m (n = 73) was measured at 19 sampling occasions at the LaoYeManQu watershed on the Chinese Loess Plateau (CLP). At a depth of 0–1.5 m, the annual mean SWS was highly correlated with rain intensity, and the correlation decreased with depth, but within the layers at 1.5–5.0 m, the changes in SWS indicated a lag between precipitation and the replenishment of soil water. Geostatistical parameters of SWS were also highly dependent on depth, and the mean SWS presented similar spatial structures in two adjacent layers. Temporal stability of SWS as indicated by mean relative difference, standard deviation of the relative difference (SDRD), and mean absolute bias error (MABE) was significantly weaker at the shallow than at deeper layers. Soil separates and organic carbon content controlled the spatial pattern of SWS at the watershed scale. One representative location (Site 57) was identified to estimate the mean SWS in the 1- to 5-m layer of the watershed. Semivariograms of the SDRD and MABE were best fitted by an isotropic spherical model, and their spatial distributions were depth-dependent. Both temporal stability and spatial variability of SWS increased over depth. This study is helpful for deep SWS estimation and sustainable management of soil and water on the CLP, and for other similar regions around the world.

KEYWORDS

deep soil, depth-dependency, geostatistics, Loess Plateau, soil–water dynamics, temporal stability

1 | INTRODUCTION

Soil–water storage (SWS) plays an important role in water cycles and energy fluxes in terrestrial ecosystems (Dobriyal, Qureshi, Badola, & Hussain, 2012; Fatichi et al., 2015; Green & Erskine, 2011; Wang, Wang, & Wang, 2017). As influenced by a series of factors including climate, soil properties, topography, land use, and the interactions among them, SWS is a highly spatial–temporal variable (Chaney, Roundy, Herrera-Estrada, & Wood, 2015; Fatichi et al., 2015; Gomez-Plaza, Martinez-Mena, Albaladejo, & Castillo, 2001; Nyberg, 1996; Regalado & Ritter, 2006). Despite this, SWS distribution often shows high spatial similarity over time. This phenomenon was referred to as temporal stability (TS; Vachaud, Passerat De Silans, Balabanis, & Vauclin, 1985), which was subsequently used to identify

representative locations for mean SWS estimation at various spatial scales (Coleman & Niemann, 2013; Hu, Shao, Han, Reichardt & Tan, 2010; Lin, 2006; Liu & Shao, 2014; Pachepsky, Guber, & Jacques, 2005; Sur, Jung, & Choi, 2013).

A majority of studies on the TS of SWS focused on the shallow layer (0–1 m), where SWS is important for modelling surface hydraulic processes, shallow-rooted plant growth, and the soil–water validation of remote sensing products at a wide range of scales (Albergel et al., 2008; Corradini, 2014; Zhu, Nie, Zhou, Liao, & Li, 2014). Many factors contribute to the TS of SWS. Depending on the scale of interest, TS of shallow SWS is controlled by meteorological conditions, topographical attributes, soil properties, and land uses (Gomez-Plaza, Alvarez-Rogel, Albaladejo, & Castillo 2000; Hu, Shao, Han, et al., 2010; Jacobs, Mohanty, Hsu, & Miller, 2004; Lin, 2006; Mohanty & Skaggs, 2001). Recently, increasing studies have been conducted to assess TS of SWS in deep soil layers below 1 m, which is essential for evaluating the response of deep-rooted plant growth to global climate change, especially to extreme drought in arid and semiarid ecosystems (Dobriyal et al., 2012; Markewitz, Devine, Davidson, Brando, & Nepstad, 2010; Steelman, Endres, & Jones, 2012; Wang et al., 2015). Deep soil water (i.e., below 1 m) supported up to 50% evapotranspiration (Volpe, Marani, Albertson, & Katul, 2013). On the Chinese Loess Plateau (CLP), rainfall and evapotranspiration were observed to influence SWS up to a depth of 2–4 m (Chen, Shao, & Li, 2008; Liu et al., 2010). Therefore, quantitative characterization of deep SWS variations is vital for assessing plant productivity and mortality and for mitigating negative effects of prolonged drought, especially in water-stressed regions such as the CLP (Jipp, Nepstad, Cassel, & De Carvalho, 1998; Rowland et al., 2015; Wang, Shao, Zhu, & Liu, 2011).

As a typical water-limited region with annual mean precipitation of 400 mm, the CLP has suffered from severe soil erosion in rainy seasons and drought stress in nonrainy seasons, which consequently resulted in low vegetation coverage, serious ecological degradation, and poor ecological function (Wang et al., 2016). To control serious soil erosion and restore the fragile eco-environment of the CLP, the "Grain for Green" programme was initiated by the Chinese government in 1999, which facilitated rapid restoration of vegetation (Chen et al., 2015; Wang et al., 2016). The wide and long-term plantations of perennial plants and exotic tree species that can utilize soil water to a depth of 5 m or deeper emphasize the importance of investigating the spatial and temporal changes in deep SWS. TS analysis, which is an effective technique to estimate SWS status, is broadly used to characterize SWS spatial distribution. Recently, research on the TS of SWS on the CLP has made great progress and has focused on detecting temporally stable locations at diverse depths (Gao & Shao, 2012; Gao, Zhao, Wu, Brocca, & Zhang, 2016; Hu, Shao, Han, et al., 2010; Jia, Shao, Wei, & Wang, 2013). Hu, Shao, Han, et al. (2010) and Gao, Wu, Zhao, Shi, and Wang (2011) identified that the TS of SWS at 0.2–0.4 m was significantly ($P < 0.05$) weaker than that at deeper depths where no significant differences in TS were found. In contrast, Gao et al. (2011) and Jia, Shao, Wei, and Wang (2013) found that TS increased with depth in the 3-m soil profile, and more time stable locations were identified in deeper layers. More recently, Gao, Shao, Peng, and She (2015) separated a soil profile into "irregularly changing" (0–0.6 m), "regularly changing" (0.6–1.6 m), and "relatively constant" layers (1.6–3.0 m) according to different TS indices. Wang et al. (2015) partitioned a 21-m soil profile into an active layer (0–2 m) and a relatively stable layer (2–21 m) based on the TS indicator. Identification of temporal stable locations in previous studies focused mainly on a single or a few numbers of sampling points, with exception of Hu, Shao, Han, et al. (2010). If spatial patterns of TS can be identified, temporally stable regions rather than points can be identified for more flexible selection of monitoring locations for estimation of mean SWS. To date, however, there are no studies that characterize the spatial patterns of TS of deep SWS due to the relatively large number of deep soil water observation that are required for geostatistical analysis. Studies on the depth-dependency and variations of deep SWS have become increasingly necessary for soil–water management and ecosystems sustainable development (Fu, Wang, Chen, & Qiu, 2003; Gao & Shao, 2012; Jipp et al., 1998; Wang, Shao, & Liu, 2013), but such information is scarce. The poor revegetation could directly lead to water scarcity in the deep-soil layer and, thus, potentially affect eco-hydrological processes. Detailed profile characteristics of deep SWS can also provide a better integrated understanding of soil–water dynamics which is valuable in hydrological applications. Understanding spatial–temporal changes in deep SWS and their depth-dependence is thus pivotal for further revegetation.

Therefore, the objectives in this study were to (a) explore the SWS dynamics of a deep profile (0–5 m) at a watershed scale and identify the temporally stable locations that could represent the mean SWS and (b) investigate the spatial patterns of SWS TS indices and controlling factors at different depths at the watershed scale.

2 | MATERIALS AND METHODS

2.1 | Description of the study area

The study was conducted at the LaoYeManQu (LYMQ) watershed (20 ha), which is located 14 km west of Shenmu County in the north part of the CLP (110°21′–110°23′E, 38°46′–38°51′N; Figure 1). Mean annual precipitation over the experimental period (2013–2015) was 437 mm, of which 70–90% fell during June–October. The annual potential evapotranspiration was 1 337 mm, and the mean annual temperature was 8.4°C, with the minimum of −23.8°C in January and the maximum of 32.5°C in July. This area was representative of the CLP, with its typical features of thick loessial deposits and deep gullies that resulted from intensive soil erosion. The uneven severe soil erosion resulted in an elevational difference of 74 m and diverse slopes that ranged from 2° to 36°. A series of steps have been taken in past decades to restore vegetation and to control soil erosion, but the local ecosystem remains fragile (Sun et al., 2015). Actual land use at the LYMQ watershed almost includes the typical vegetation on the CLP and has been further categorized into eight types, which are based on the dominant species and extent of coverage (Hu, Shao, Han, et al., 2010; Figure 1b). The number of sampling locations in Poplar, sand korshinsk peashrub, mixed shrub, farm land, grassland, almond, dense korshinsk peashrub, and sparse korshinsk peashrub are 5, 5, 4, 11, 24, 3, 10, and 11, respectively. Aeolian sandy soils

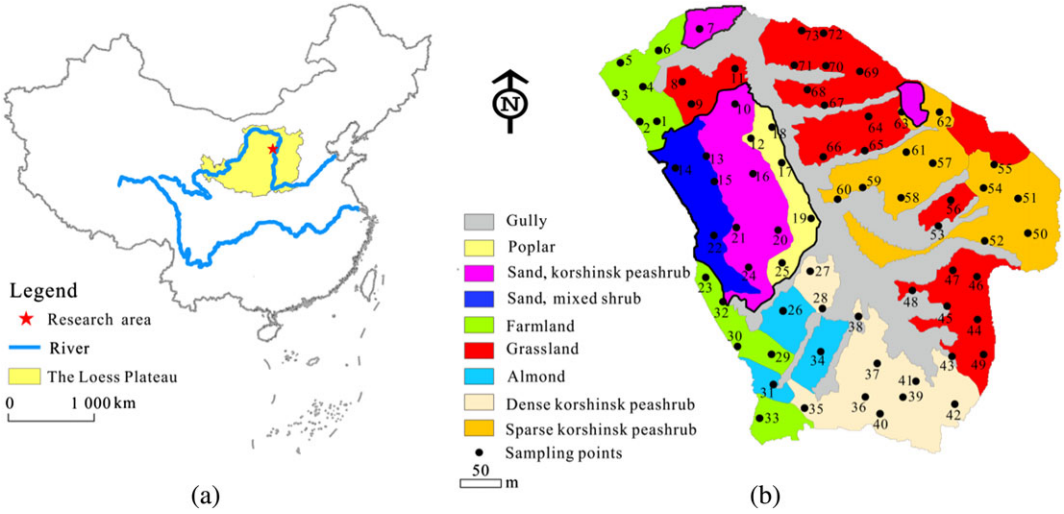

FIGURE 1 The location of the study area in China (a) and the sampling points in the LaoYeManQu watershed (b).The area bordered by the black line contains Aeolian sandy soils, and the other areas contain Ust-Sandiic Entisol soils

(composed of sand or loamy sand) and Ust-Sandiic Entisol soils (which are dominated by sandy or silty loam) in the watershed are also common across the CLP (Figure 1). Soil stratification (the A horizon at 0.1–0.3 m depth contained a large amount of soil organic matter, and the C horizon has parental materials) has been identified in soil profiles for both soil types, despite the distinct content of alluvial $CaCO_3$ that was distributed widely in the C horizon of the Ust-Sandiic Entisol soils (Hu, Shao, & Reichardt, 2010).

2.2 | Sampling locations and data collection

Five metre-long aluminium neutron probe access tubes were installed in fall 2012 at 73 locations to monitor soil water content. The 73 locations were selected from a 50 m × 50 m grid. The installations were stabilized for 6 months before low-neutron counting rates (CRs) were retrieved at 0.1 and 0.2 m intervals in the 0–1 and 1–5 m layers, respectively, on 19 sampling dates from May 18, 2013, to October 28, 2015. Disturbed soil samples up to a depth of 5 m were sampled with a 0.05-m diameter soil corer at each location during the aluminium tube installation. Five hundred eighty-four soil samples were collected from eight layers (i.e., 0–0.1, 0.1–0.2, 0.2–0.6, 0.6–1.0, 1.0–2.0, 2.0–3.0, 3.0–4.0, and 4.0–5.0 m) to determine soil particle composition using the MasterSizer2000 apparatus and to determine soil organic carbon content using the dichromate oxidation method (Nelson & Sommers, 1975). Undisturbed soil samples at a 0.05-m height (0.05 m in diameter) near each location were also collected to measure saturated hydraulic conductivity (Ks) and bulk density (BD) using the constant head method and the gravimetrical method, respectively. Meteorological data, which included precipitation, relative humidity, wind speed, and temperature, were obtained automatically with a weather monitoring system (ZK-NT10A) on a flat field on a mountain top.

Gravimetric soil water content (SWC; GSWC, g H_2O/100 g dry soil, %) and BD were further measured to calibrate the neutron probes at eight different sites that covered the entire watershed to ensure that all soil textures and land-use types in the area were represented. The direct measurement of BD within a 5-m profile was difficult; thus, only 1-m depth pits were excavated at each calibration location near the neutron tubes to collect undisturbed soil samples for BD determination, which was used to transform the GSWC into volumetric SWC (VSWC, cm^3/cm^3). The GSWC and BD ranged from 0.8% to 22.5% and 1.00 to 1.71 g/cm^3, respectively. Both were within the ranges of GSWC and BD measured in the watershed generally, which indicated that the locations were representative for establishing the calibration equations. With the calibration curve, VSWC could be derived from the values of the CRs that were measured directly by the neutron probe. The corresponding calibration curve equation can be written as

$$\mathrm{VSWC} = 62.233\mathrm{CR} + 0.9459 \left(R^2 = 0.92, P<0.001\right). \quad (1)$$

Then, the SWS at site i, time j, and depth k (SWS_{ijk}, mm) was calculated from the corresponding VSWC and the selected depth. SWS_{ij} for each 0.5-m soil layer up to 5-m depth was calculated to assess vertical distribution of SWS and temporal dynamics. TS and depth-dependency were evaluated further by using the standard deviation of the relative difference (SDRD; Vachaud et al., 1985) and the mean absolute bias error (MABE; Hu, Shao, & Reichardt, 2010).

2.3 | Statistical methods

2.3.1 | Temporal stability analysis

Two indices were used to access TS. The first method refers to the SDRD and mean relative difference (MRD) introduced by Vachaud, Passerat De Silans, Balabanis, and Vauclin (1985). The SDRD, or the combination of MRD and SDRD, can both generally characterize TS. Specifically, the lower the MRD and SDRD, the more stable a location. Generally, a location with MRD and SDRD <5% is considered to be temporal stable. The index of temporal stability (ITS) deduced from the SDRD and MRD can be calculated (Jacobs

et al., 2004) to identify a temporally stable location. Usually, a location with an ITS value <10% can be used directly to represent mean SWS across the entire watershed (Zhao, Peth, Wang, Lin, & Horn, 2010).

The MABE was another index introduced by Hu, Shao, and Reichardt (2010) to evaluate TS. The underlying distinction between SDRD and MABE is that the latter can be used directly to represent the time-averaged, bias error using an identified location to produce the mean SWS. A MABE value <5% is selected as the criterion for identifying locations to estimate mean SWS in the LYMQ watershed.

2.3.2 | Geostatistical analysis

Semivariograms used to characterize spatial patterns of SWS, SDRD, and MABE can be calculated as

$$\gamma(h) = \frac{1}{2N(h)} \sum [z(x) - z(x+h)]^2, \quad (2)$$

where $\gamma(h)$ and h are the semivariogram and lag distance, respectively. N (h) is the number of pairs of samples separated by h, and z (x) and z (x + h) are the measured values of variables (i.e., SWS, SDRD, and MABE) at the associated locations x and x + h, respectively (Feng, Liu, & Mikami, 2004). Four theoretical semivariogram models (i.e., linear, spherical, exponential, and Gaussian) were used to fit the obtained empirical semivariograms to produce geostatistical parameters. Details on different theoretical models can be found in Nielsen and Wendroth (2003). Generally, a nugget–sill ratio ≤25% indicates a strong spatial dependency, a ratio ≥75% indicates a weak spatial dependency, and an intermediate ratio indicates a moderate spatial dependency (Nielsen & Wendroth, 2003). Based on the semivariance analysis, the spatial distribution of SWS, SDRD, and MABE in various soil layers were estimated using ordinary kriging.

2.4 | Data analysis

Classical statistics that included mean, standard deviation (*SD*), and coefficient of variation (CV) of SWS were calculated for various layers. The degree of variation was evaluated by the CV value. Generally, variability was considered low, moderate, and strong at CV < 10%, 10% ≤ CV ≤ 100%, and CV > 100%, respectively (Hu, Shao, Han, et al., 2010). The *t* test was used to determine if the differences were statistically significant.

3 | RESULTS AND DISCUSSION

3.1 | Traditional spatial–temporal analysis of soil–water storage

3.1.1 | Basic characteristic of mean soil–water storage

The time-averaged mean SWS at 0.5 m depths generally increased with depth, from 57.2 (0–0.5 m) to 70.6 mm (4.5–5.0 m). There was a significant difference (P < 0.05) of SWS between 0 and 0.5 m and other layers (Table 1). The SD_S and CV_S over space of mean SWS increased with depth, which indicated that SWS in deeper soil layers had greater spatial variability. However, spatially averaged CV and SD over time (i.e., CV_T and SD_T) varied moderately (10% < CV < 100%) at a depth of 0–0.5 and 0.5–1 m and varied weakly (CV < 10%) in deeper layers, which suggested that temporal variability of SWS tended to decrease with depth. These results are consistent with previous observations by Gomez-Plaza et al. (2001), Brocca, Melone, Moramarco, and Morbidelli (2009), Hu, Shao, Han, et al. (2010), Jia et al. (2013), Corradini (2014), and Fatichi et al. (2015). In this study, the weak temporal variability of SWS within the deep layers at 1–5 m can be ascribed to the small influence of precipitation and evapotranspiration, with the exception of water uptake by some perennial deep-rooted plants, such as Peashrub (Chen et al., 2008). Whereas, the strong spatial variability in deep layers was due to the

TABLE 1 Basic statistics of soil–water storage (SWS) from 2013 to 2015 at various soil depths on the Chinese Loess Plateau, China

Spatial variables	Temporal statistic	Soil layer (m)									
		0–0.5	0.5–1.0	1.0–1.5	1.5–2.0	2.0–2.5	2.5–3.0	3.0–3.5	3.5–4.0	4.0–4.5	4.5–5.0
Mean SWS	Min, mm	34.1	50.2	55.4	55.9	54.6	53.4	54.2	54.5	57.2	60.5
	Max, mm	83.9	84.5	83.5	78.5	72.6	69.6	6.9.1	68.4	69.3	73.4
	Mean, mm	57.2§[a]	64.6[b]	64.8[b]	66.3[b]	65.9[b]	64.9[b]	65.8[b]	65.5[b]	66.8[b]	70.6[b]
	SD_T, mm	12.0	10.1	6.5	5.1	4.2	3.8	3.5	2.9	2.5	2.6
	CV_T, %	21.0	15.6	9.9	7.8	6.4	5.9	5.3	4.5	3.7	3.7
SDs of SWS	Min, mm	12.0	18.7	20.8	21.4	22.1	20.8	21.7	22.5	22.9	25.6
	Max, mm	28.6	33.7	31.7	30.1	30.6	28.5	29.9	29.1	28.3	32.7
	Mean, mm	20.4	24.6	26.7	27.5	27.6	26.1	27.7	27.5	27.0	30.3
	SD_T, mm	5.3	3.7	2.9	2.1	1.8	1.8	1.9	1.5	1.2	1.4
	CV_T, %	25.7	15.1	10.8	7.7	6.6	6.7	6.8	5.6	4.3	4.8
CVs of SWS	Min, %	26.2	30.9	34.1	38.3	39.9	38.6	40.1	40.4	39.7	41.5
	Max, %	45.0	45.9	45.7	44.2	44.2	41.9	43.8	43.7	41.9	44.8
	Mean, %	35.8	38.3	41.2	41.5	41.9	40.2	42.0	42.0	40.5	42.9
	SD_T, %	6.0	4.1	3.3	1.6	1.2	0.9	1.0	0.9	0.6	0.8
	CV_T, %	16.7	10.7	7.9	3.8	2.8	2.6	2.4	2.1	1.4	2.0

Note. The SDs of SWS represent the standard deviation of the spatial SWS, the CVs of SWS represent the coefficient of variation of the spatial SWS, the SD_T represents the standard deviation of the time series based on the mean spatial SWS, and the CV_T represents the coefficient of variation for the time series based on mean spatial SWS. Different letters indicate significant differences, and § represents significantly different values, with P < 0.05.

accumulative effects of rainfall infiltration and run off, which were controlled primarily by soil properties, topography-related factors, and land use types (Smith, Bracken, & Cox, 2010).

3.1.2 | Dynamics of soil–water storage

The annual precipitation was 631,438,336 mm in 2013, 2014, and 2015, respectively (Figure 2). This indicated that 2013 was much wetter than the other 2 years. Large fluctuations in SWS existed within the layers at 0–0.5 and 0.5–1.0 m as a result of their rapid response to rainfall and evapotranspiration. SWS at a depth of 1.0–1.5 m also responded to meteorological conditions (e.g., excessive rainfall in 2013 and drought in 2015), whereas we identified only slight changes in SWS below 1.5 m, except for a sharp oscillation that occurred with heavy rainstorms in 2013.

The SWS balance is dictated by a combination of prevailing water and energy balances (Gomez-Plaza et al., 2001). Likewise, deep SWS dynamic patterns are controlled predominantly by infiltration, groundwater recharge, and water uptake by deep-rooted vegetation (Huang & Pang, 2011; Lin, 2006; Smith et al., 2010; Volpe et al., 2013). The groundwater was very deep (>50 m) in this study area. Therefore, the upsurge of deep SWS in 2013 could be ascribed to the accumulative infiltration that resulted from the heavy rainstorms during the wet season, and the reduction of the SWS may be attributed to substantial water uptake by deep-rooted vegetation (e.g., Poplar and Peashrub) and water redistribution to deeper layers. Due to water shortages, most vegetation in the watershed was identified as the "little old man tree" (i.e., trees with withered treetop), which indicated lower physiological vitality and weaker ecological function. In fact, alteration in precipitation patterns cause shifts in net primary production and root biomass. This resulted in changes in eco-hydrological processes and soil water balance at diverse soil depths (Sarris, Christodoulakis, & Korner, 2007). However, this alteration in deep SWS needs further verification by a tracer test using a radioactive isotope such as $^{3}H_2O$ (Huang, Pang, & Edmunds, 2013).

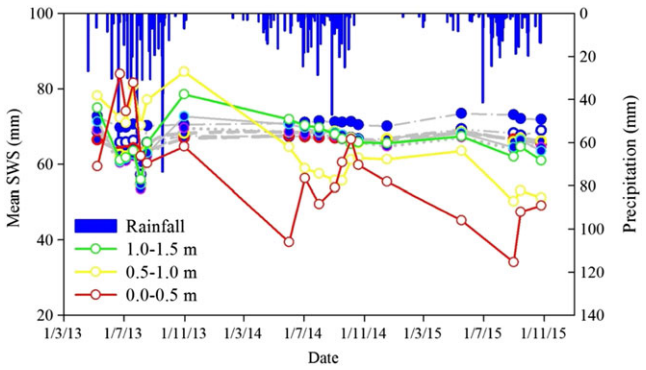

FIGURE 2 Dynamics of the mean SWS and precipitation from May 18, 2013, to October 28, 2015 in the watershed on the Chinese Loess Plateau, China. Grey curves represent soil–water storage (SWS) in the 2- to 5-m layer. Points represent the mean SWS spatially at each measurement date. The lines that connect the measurement points are intended for visualization and do not represent actual SWS changes between the measurement dates

3.1.3 | Spatial distribution of soil–water storage

The semivariograms showed that SWS approached a stable sill at certain lag distances (Table 2). The spherical variogram model was well fitted to describe the experimental semivariance of SWS in various layers. The geostatistical parameters varied with depth. Specifically, the nugget variance and sill variance increased with depth, which indicated the stronger SWS variability within deeper soil layers. The nugget–sill ratio was <25% within the layers at 0–0.5, 0.5–1.0, 1.0–1.5, 1.5–2.0, and 2.0–2.5 m and 25–75% for the other layers, which implied that SWS were strongly and moderately spatially dependent at the depth of 0–2.5 and 2.5–5.0 m, respectively. The range (i.e., spatial autocorrelation distance) of SWS for the upper 1.0 m was 163 m, which is comparable to those of 0–0.8 m (i.e., 151–186 m) observed by Hu, Shao, Han, et al. (2010). With increasing soil depth, the range of SWS generally decreased. Interestingly, the range of SWS at a depth of 2.5–3.5 m (104–124 m) was similar to that of the total vegetation yield (122 m) reported by Hu, Shao, Han, et al. (2010). This may imply that the spatial pattern of SWS in these layers is closely associated to the water uptake by deep-rooted vegetation.

Temporal mean SWS exhibited similar spatial patterns in adjacent soil layers (Figure 3). This was supported by Pearson correlation coefficients (R = 0.8–0.95, P < 0.01) between adjacent soil layers. SWS

TABLE 2 Geostatistical analysis of mean soil–water storage for various soil layers on the Chinese Loess Plateau, China using the spherical variogram model

Soil layer (m)	Nugget variance	Sill variance	Range (m)	Structured variance	Nugget–sill ratio (%)	r^2	Kolmogorov–Smirnov test
0–0.5	84	434.3	163.4	350.3	19.3	0.89	0.90
0.5–1.0	110	678.3	164.4	568.3	16.2	0.78	0.87
1.0–1.5	122	801.7	152.7	679.7	15.2	0.82	0.75
1.5–2.0	142	847.8	140.2	705.8	16.7	0.80	0.79
2.0–2.5	159	845.6	134.5	686.6	18.8	0.80	0.54
2.5–3.0	201	748.8	124.6	624.2	26.8	0.82	0.64
3.0–3.5	211	836.0	104.3	731.7	25.2	0.78	0.20
3.5–4.0	328	818.1	96.0	722.1	40.1	0.74	0.63
4.0–4.5	398	791.5	92.1	699.4	50.3	0.78	0.72
4.5–5.0	441	974.0	91.1	882.9	45.3	0.78	0.70

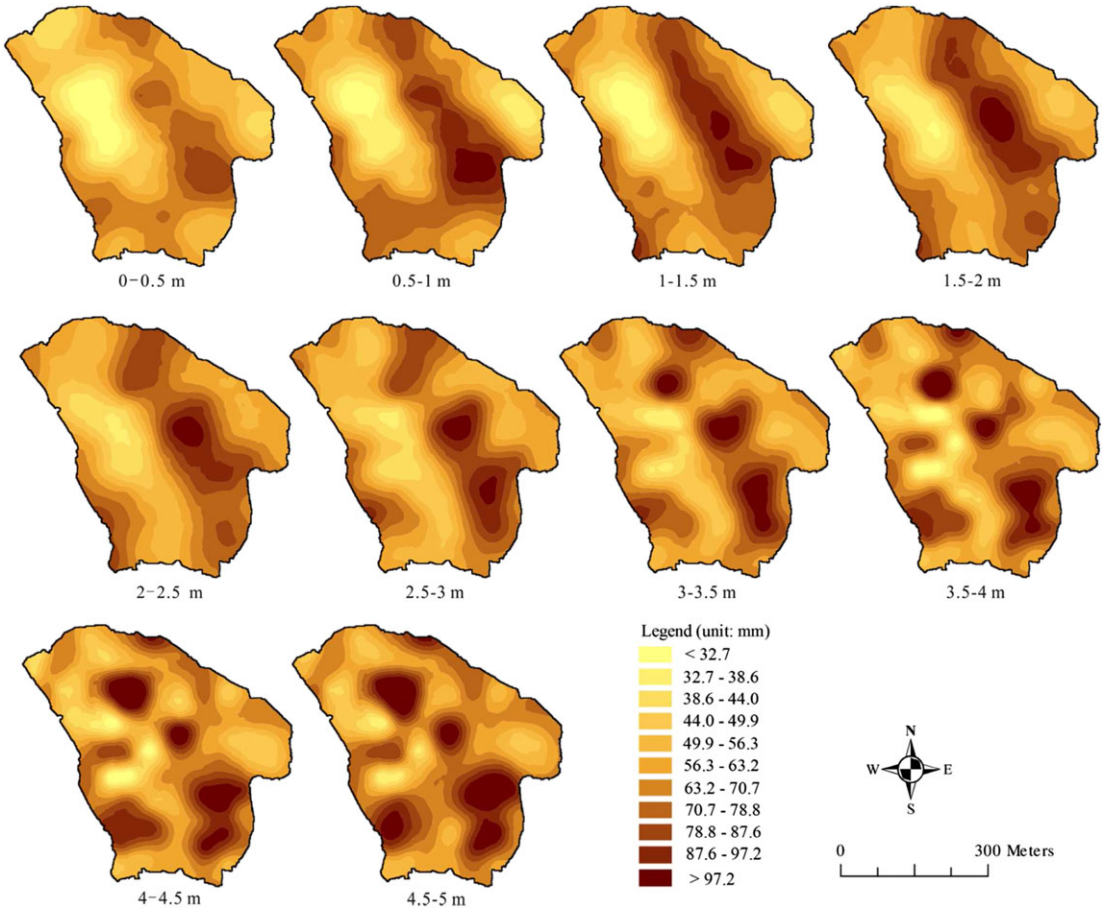

FIGURE 3 Distribution of mean soil–water storage in various soil layers on the Chinese Loess Plateau, China

within the layers at 0–3.0 m was higher on southwest-facing slopes than that in of northeast-facing slopes where sand or loamy sand dominated. The contrasting SWS at the depth of 0–3.0 m on different slopes could be attributed to the soil separates diversion. The area with lowest SWS on the northeast-facing slopes became wetter with depth beyond 3.0 m. Improved soil water-holding capability as a result of enhanced clay content may be the reason (Wang et al., 2015). Some higher SWS existed in the deep layers of the gully due to the vertical hydrological flux in wet surface areas (Gannon, Bailey, & McGuire, 2014). During the rainy seasons, topography was a major factor that promoted the deep SWS accumulation through surface and subsurface run-off (Lin, 2006).

TABLE 3 The associated parameters of mean soil–water storage (SWS) for various soil layers on the Chinese Loess Plateau, China

		Soil layer (m)									
Parameter		0–0.5	0.5–1	1–1.5	1.5–2	2–2.5	2.5–3	3–3.5	3.5–4	4–4.5	4.5–5
MRD (%)	Min	−55.3	−61.6	−62.6	−62.5	−68.8	−66.9	−66.2	−65.9	−65.7	−66.6
	Max	69.7	82.7	94.4	98.9	102.7	84.1	126.2	157.6	154.3	149.2
	Range	125.0	144.2	156.9	161.3	171.5	151.0	192.4	223.6	220.0	215.8
	N_a	7	4	4	6	8	9	10	8	8	7
SDRD (%)	Min	4.8	3.3	3.1	3.0	1.7	2.6	1.6	1.1	1.5	0.9
	Max	22.3	24.1	24.5	35.5	35.6	27.8	26.7	18.8	15.2	12.7
	Mean	12.1	9.5	9.4	9.1	8.4	7.5	6.9	5.8	4.8	4.5
	Range	17.5	20.8	21.5	32.4	33.8	25.2	25.1	17.7	13.8	11.8
	N_b	1	4	8	12	13	25	30	42	45	47
MABE (%)	Min	3.9	3.3	2.4	2.6	2.1	1.6	1.5	1.9	1.7	1.5
	Max	31.2	25.6	36.3	29.4	28.6	22.6	20.2	14.3	30.2	25.3
	Mean	10.6	8.5	9.1	8.3	7.5	6.6	5.8	4.8	4.4	4.2
	Range	27.4	22.3	33.9	26.8	26.5	21.0	18.8	12.4	28.5	23.8
	N_c	6	15	17	27	28	32	42	54	58	60

Note. The mean relative difference in soil–water storage is represented by MRD, and the two different indexes (SDRD and MABE) are corresponding surrogates to the standard deviation of the relative difference and the mean absolute bias error, respectively. N_a represents the number of locations with MRDs from −5% to +5%. N_b and N_c are the number of locations with SDRD and MABE <5%, respectively.

3.2 | Temporal stability of soil–water storage and its influencing factors

3.2.1 | Temporal stability of soil–water storage at the watershed scale

The MRD ranges generally increased with depth, which echoed the stronger spatial variability at a depth of 3.5–5.0 m that was also reflected by the greater sill variance (Table 3 and Figure 4). The MRD ranges in this study were greater than others (Jia et al., 2013; Zhao et al., 2010). This can be ascribed to higher heterogeneity of soil type, land use types, and topographical attributes across the watershed (Wang et al., 2015).

SDRD and MABE have been used widely to evaluate the TS of SWS. In this study, associated time-averaged SDRD and MABE decreased with increasing depth (Table 3). These results were consistent with previous studies (Hu, Shao, & Reichardt, 2010; Gao et al., 2011; Jia et al., 2013). The number of temporally stable locations increased with increasing depth. For example, the numbers of the

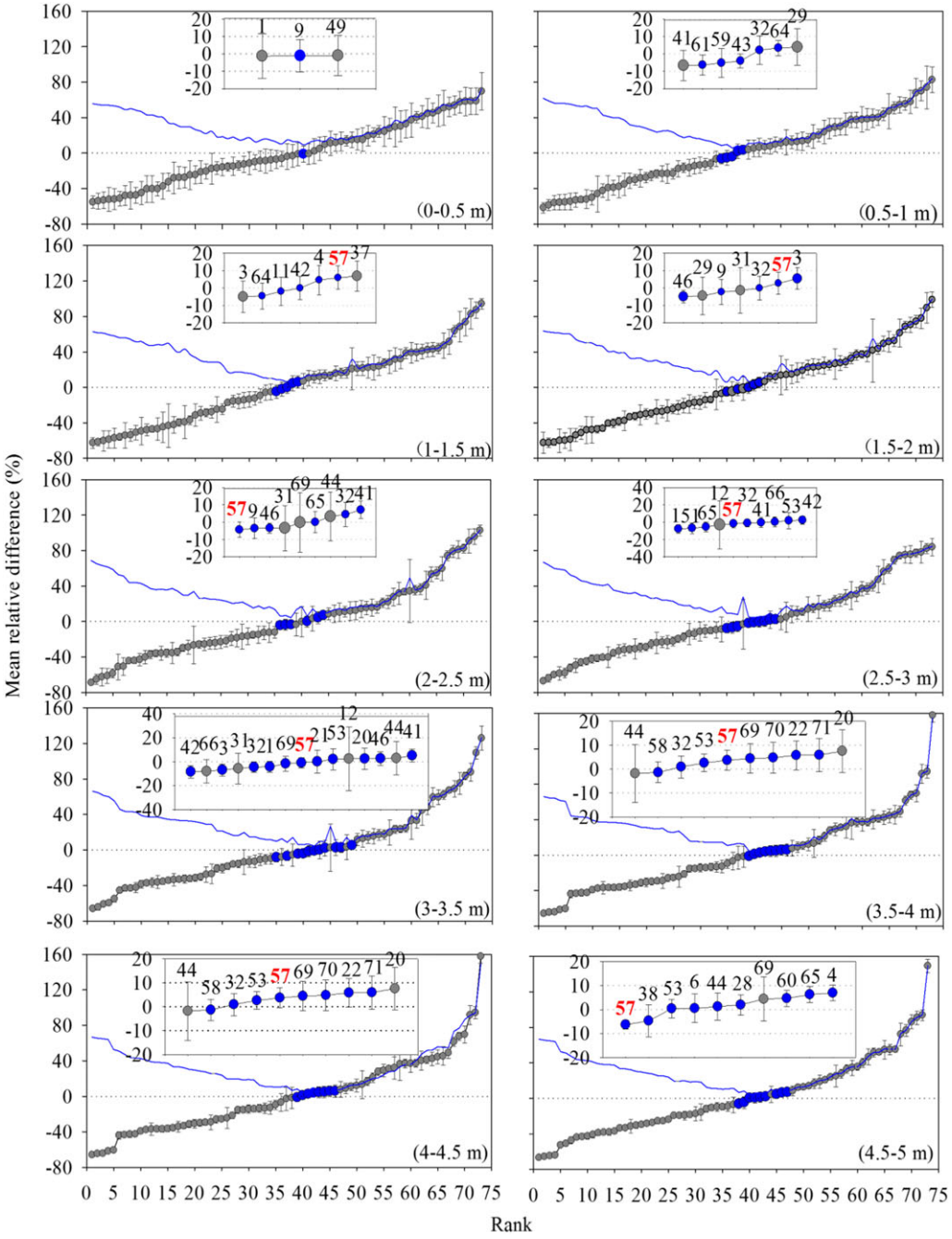

FIGURE 4 Ranked mean relative differences (MRD) in soil–water storage and the index of temporal stability (ITS) for all soil layers at all sampling locations in LaoYeManQu watershed on the Chinese Loess Plateau, China. Vertical bars represent ±one standard deviation in relative differences. The blue curves indicate the ITS, and locations with an ITS <10% are marked with blue circles. The red number above the corresponding blue circles represents the single common location representative of the temporal stability

locations with SDRDs and MABEs <5% were 1 and 6 at the depth of 0–0.5 m and 47 and 60 at the depth of 4.5–5.0 m, respectively. These results indicated a stronger TS of SWS at deeper layers due to the smaller influence of climate (Wang et al., 2015).

If ITS values <10% are acceptable for estimation of mean SWS, there were 1, 5, 5, 5, 6, 9, 11, 8, 8, and 9 temporally stable locations from 0–0.5 to 4.5–5.0 m, respectively (Figure 4). Only Location 9 approximately reflected mean SWS within the layer at 0–0.5 m. The increased number of temporally stable locations with depth was attributed to the less involvement of hydrological processes, which included lateral run-off, infiltration, and evapotranspiration in deeper layers (Wang, 2012). Finding a single common location to represent the mean SWS for multiple layers was difficult (Vanderlinden et al., 2012) but was an advantage for the efficient evaluation of deeper SWS (Hu, Shao, Han, et al., 2010; Jia et al., 2013; Martinez-Fernandez & Ceballos, 2003). Although no single representative locations were identified for the complete soil profile, we found that Location 57 can be used to represent mean SWS at a depth of 1–5 m.

Using a single location to represent mean SWS in deeper layers may be cost effective by sacrificing, to some extent, the accuracy of the SWS prediction. Therefore, relationships between the measured SWS at the representative locations and the mean values for the entire watershed were plotted to assess the reliability of the estimation (Figure 5). With a few exceptions, most of the selected temporally stable locations represented the mean SWS for the watershed within a margin of 5% between 0 and 2.0 m, as did Location 57 below 2 m. Moreover, the plot of mean SWS compared to SWS at representative locations (Figure 5) showed that the selected representative locations for the 2.0- to 5.0-m layers could be better used to assess mean SWS than that above 2 m. Compared to other studies that were conducted at point, slope, or transection scales (Jia et al., 2013; Liu & Shao, 2014), our study demonstrated a lower feasibility of using temporally stable locations to predict mean SWS at a watershed scale. In addition, temporally stable locations identified from 0 to 2.0 m highly overestimated or underestimated mean SWS with offset >5%; by contrast, the representative locations identified below 2 m estimated mean SWS values within 5% offset at each sampling date. This could be ascribed to the lower sensitivity of SWS to precipitation and evaporation at selected representative locations for deeper layers (Jia et al., 2013; Tague, Band, Kenworthy, & Tenebaum, 2010). Notwithstanding, the temporally stable locations that we selected were beneficial for estimating mean SWS because of the reduction in the required number of samples and acceptable accuracy of the prediction.

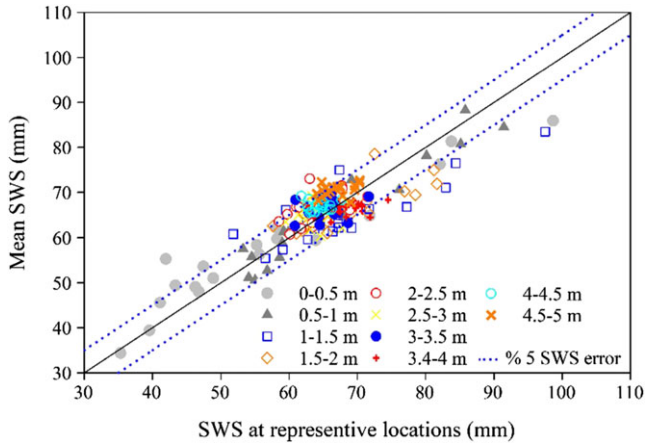

FIGURE 5 Relationships between mean soil–water storage (SWS) and measured SWS at representative locations for various soil layers in LaoYeManQu watershed, where selected representative locations in the corresponding layer at depths of 0–0.5, 0.5–1, and 1–5 m were Locations 9, 64, and 57, respectively. Blue dotted line represents the 5% of SWS error

3.2.2 | Factors that influence soil–water storage

Previous studies found that soil properties, topography, land use type, and antecedent/saturation soil moisture affected SWS (Fu et al., 2003; Gao & Shao, 2012; Jacobs et al., 2004; Mohanty & Skaggs, 2001). Correlation analyses showed that soil separates and soil organic carbon content were the main determinants of MRD in different layers (Table 4). For example, sand and clay contents were negatively correlated and positively correlated to SWS, respectively, which is in agreement with Hu, Shao, Han, et al. (2010) and Martinez-Fernandez

TABLE 4 Pearson correlation coefficients between mean relative differences (MRDs) in soil–water storage and corresponding variables on the Chinese Loess Plateau, China

	MRD in the soil layers (unit: m)							
Parameter	0–0.1	0.1–0.2	0.2–0.6	0.6–1	1–2	2–3	3–4	4–5
Elevation	0.23	0.26[a]	0.22	0.18	0.12	0.06	−0.09	−0.18
BD	−0.43[b]	−0.48[b]	−0.46[b]	−0.43[b]	−0.33[b]	−0.19	−0.12	−0.09
Ks	−0.65[b]	−0.65[b]	−0.60[b]	−0.57[b]	−0.49[b]	−0.36[b]	−0.21	−0.11
Clay	0.74[b]	0.79[b]	0.87[b]	0.84[b]	0.82[b]	0.62[b]	0.60[b]	0.74[b]
Silt	0.77[b]	0.81[b]	0.78[b]	0.77[b]	0.76[b]	0.64[b]	0.64[b]	0.54[b]
Sand	−0.77[b]	−0.81[b]	−0.80[b]	−0.79[b]	−0.79[b]	−0.65[b]	−0.65[b]	−0.64[b]
SOC	0.30[a]	0.48[b]	0.35[b]	0.26[a]	0.49[b]	0.49[b]	0.44[b]	0.47[b]

Note. BD and Ks were measured for the 0- to 5-cm soil layer and represent the bulk density and saturated hydraulic conductivity, respectively. SOC represents soil organic carbon.

[a]Indicates that the correlation was significant at the 0.05 level (2-tailed test).

[b]Indicates that the correlation was significant at the 0.01 level (2-tailed test).

and Ceballos (2003). Moreover, soil surface hydraulic properties such as BD and Ks also contributed to the spatial distribution of SWS throughout the entire soil profile through their impacts on soil water retention and infiltration rate. However, Jia et al. (2013) found that MRD was not correlated with Ks but was positively correlated with BD. This was possibly due to the lower variability of Ks at a slope scale in the study of Jia et al. (2013). In general, topography controlled SWS distribution in areas surface run-off dominated (Grayson, Bloschl, Western, & McMahon, 2002; Lin, 2006). In this study, a weak effect of elevation on MRD was found because vertical flux that was driven by evapotranspiration was the dominant process in this area (Wang et al., 2015). Furthermore, lateral flow that was controlled by higher

TABLE 5 Geostatistical analysis of the standard deviation of relative difference (SDRD) and the mean absolute bias error (MABE) of SWS for difference soil layers (spherical model) in the LaoYeManQu watershed on the Chinese Loess Plateau

	SDRD					MABE				
Soil layer (m)	Nugget variance (%^{2})	Sill variance (%^{2})	Range (m)	Nugget–sill ratio (%)	R^2	Nugget variance (%^{2})	Sill variance (%^{2})	Range (m)	Nugget–sill ratio (%)	R^2
0–0.5	4.4	14.9	72	30	0.89	11.2	28.3	178	40	0.93
0.5–1	3.8	14.6	80	26	0.72	3.7	25.6	176	14	0.93
1–1.5	7.4	19.8	79	37	0.77	16.6	57.4	170	29	0.97
1.5–2	10.0	24.3	57	41	0.47	20.6	39.1	183	53	0.92
2–2.5	9.0	22.2	98	40	0.52	13.6	27.2	156	50	0.89
2.5–3	6.5	19.2	81	34	0.46	9.2	16.2	114	57	0.62
3–3.5	3.9	19.0	69	20	0.56	6.2	12.0	107	52	0.58
3.5–4	2.8	12.2	83	23	0.91	4.5	9.0	96	50	0.68
4–4.5	1.8	7.5	95	24	0.84	4.1	14.7	83	28	0.81
4.5–5	1.2	7.2	87	16	0.72	2.0	11.1	80	18	0.75

Note. Nugget variance, sill variance, range, and nugget–sill ratio are geostatistical parameters; nugget–sill ratio represents degree of spatial dependence; and R^2 represents fitting degree of spherical variogram model.

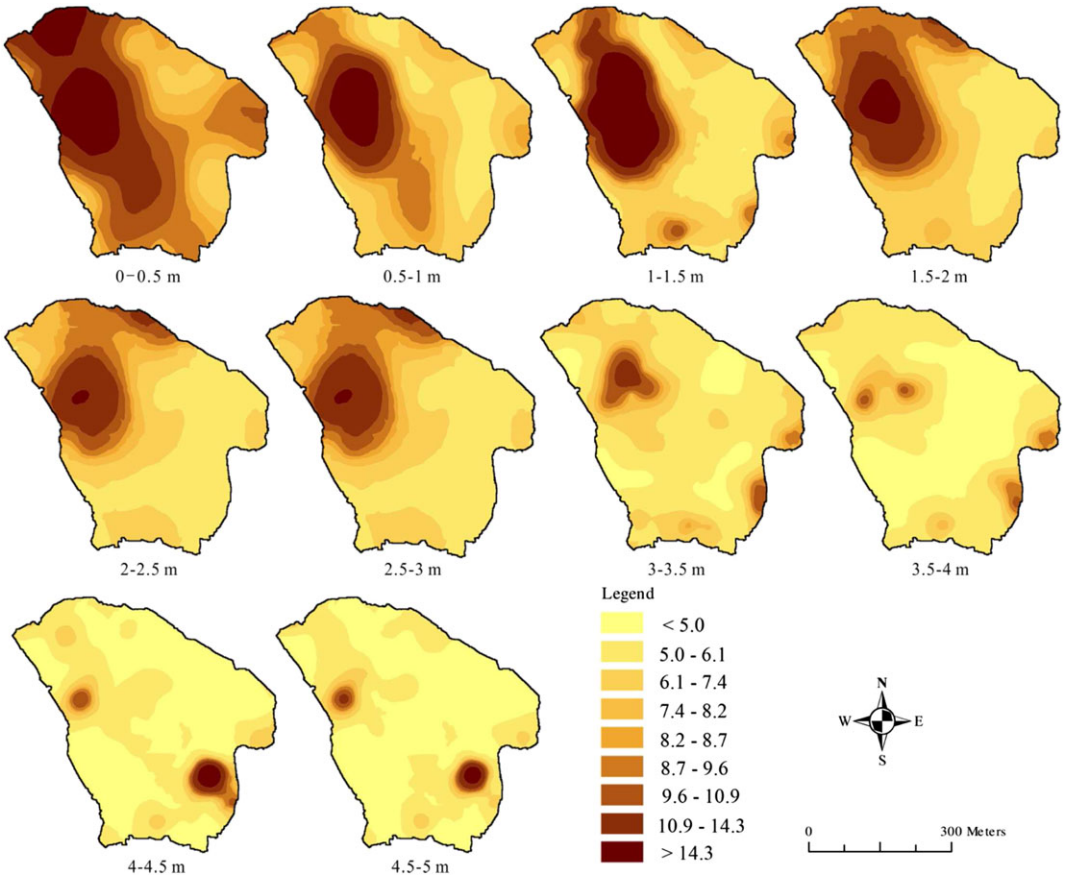

FIGURE 6 Spatial patterns of the standard deviation of the relative difference (%) for soil–water storage in various soil layers in the LaoYeManQu watershed on the Chinese Loess Plateau, China

saturated horizontal conductivity and soil horizon in the wet seasons facilitated high deep SWS in valleys (Coleman & Niemann, 2013). Land use types also strongly controlled deep SWS through evapotranspiration, which can be affected by root distribution, plant density, and species diversity (Zhao et al., 2010). In addition, land use types affected SWS through their impacts on soil water retention and hydraulic conductivity (Lv, Liao, Lai, Zhu, & Zhou, 2016).

3.3 | Geostatistical analysis of temporal stability indices of soil–water storage

The semivariances for SDRD and MABE approximated a stable plateau at a certain distance, which was fitted well by a spherical model (Table 5). The nugget and sill variance of SDRD and MABE were the highest in the 1.0- to 2.0-m layer and generally decreased with depth until 4.0–5.0 m where the lowest values were observed. This indicated that variability of TS was the greatest within the layers at 1.0–2.0 m. The nugget–sill ratio of SDRD and MABE showed no regular trend with depth, although SDRD ranged from 26% to 41% (0–3.0 m) and 16–24% (3.0–5.0 m), which indicated medium and strong spatial dependency, respectively. The range of MABE decreased with increasing depth and was greater than the range of SDRD at the depth of 0–4.0 m, which suggested that the MABE was spatially correlated in a broader domain than SDRD within the layers at 0–4.0 m.

Sites near the temporally stable locations tended to be temporally stable, which suggested that there was an extended temporally stable area (Hu, Shao, Han, et al., 2010). Spatial patterns of SDRD and MABE in consecutive layers (Figures 6 and 7) were nearly coincident, which was supported by the Pearson correlation coefficients ($P < 0.01$). Pearson correlation coefficients for SDRD increased from 0.48 to 0.87 then stabilized in deeper layers, which implied that there was a higher similarity among deeper layers. Likewise, Pearson correlation coefficients for MABE consistently maintained a higher level from 0.59 to 0.95. Therefore, TS identified by the SDRD and/or MABE increased with depth, with the exception of some sandy soil areas and dense korshinsk peashrub land (Figure 1).

The vertical distribution of mean SWC at the watershed scale differed greatly in the soil profile over 3 years, but the differentiation was negligible in deeper (>2.4 m) layers (Figure 8). Because groundwater was too deep (>50 m) to be involved in the hydrological processes in the CLP, water uptake by deep roots and water redistribution from rainfall were the main influences on the deep SWS (Mu, Zhang, McVicar, Chille, & Gau, 2007). The consistent SWC below 2.4 m over 3 years may indicate that water redistributed into deeper soils was lifted up via water uptake by root. Based on the TS analysis, temporally stable Location 57 was used to predict annual changes in deep SWC (>1 m). For each year, SWC of Location 57 and mean SWC at the watershed scale were comparable beyond 2.4 m with SWC differences less than 1% (Figure 8). This again indicates that Location 57 can be used not only for representing mean SWS of deeper (>1 m) layers but also for capturing the vertical distribution of watershed SWC at deeper layers.

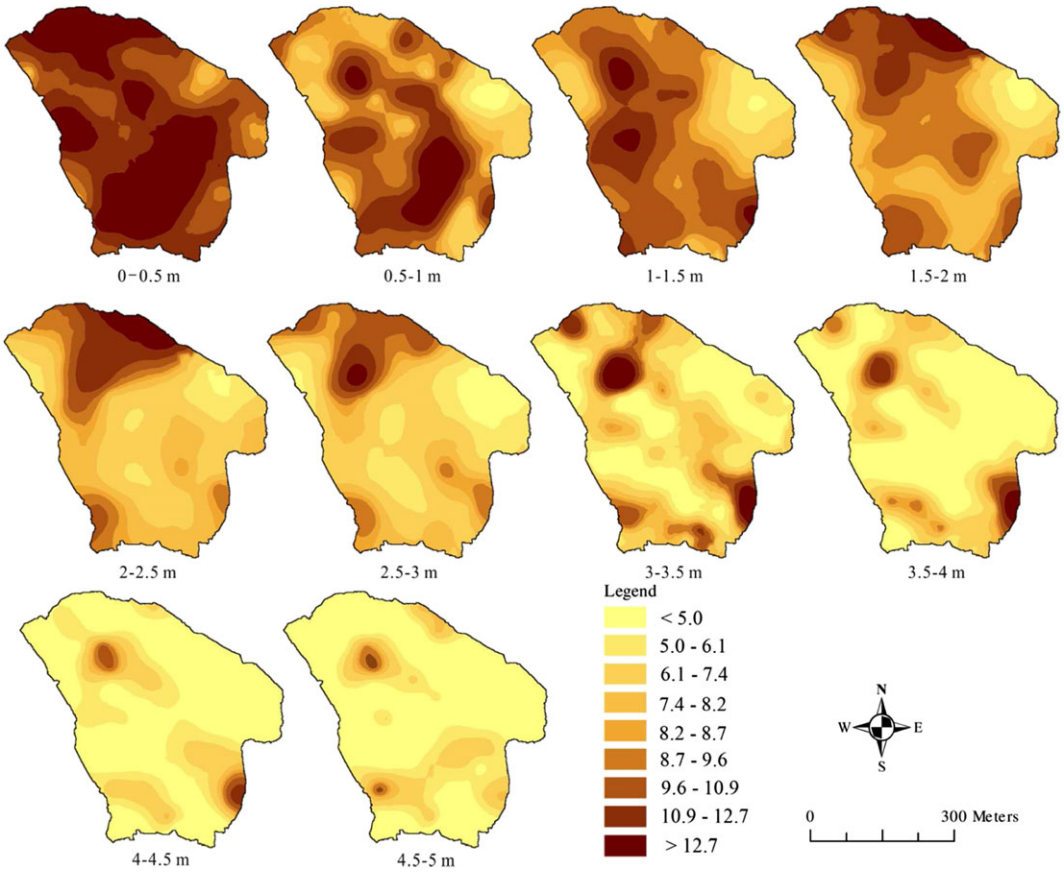

FIGURE 7 Spatial patterns of mean absolute bias errors (%) for soil–water storage in various soil layers in the LaoYeManQu watershed on the Chinese Loess Plateau, China

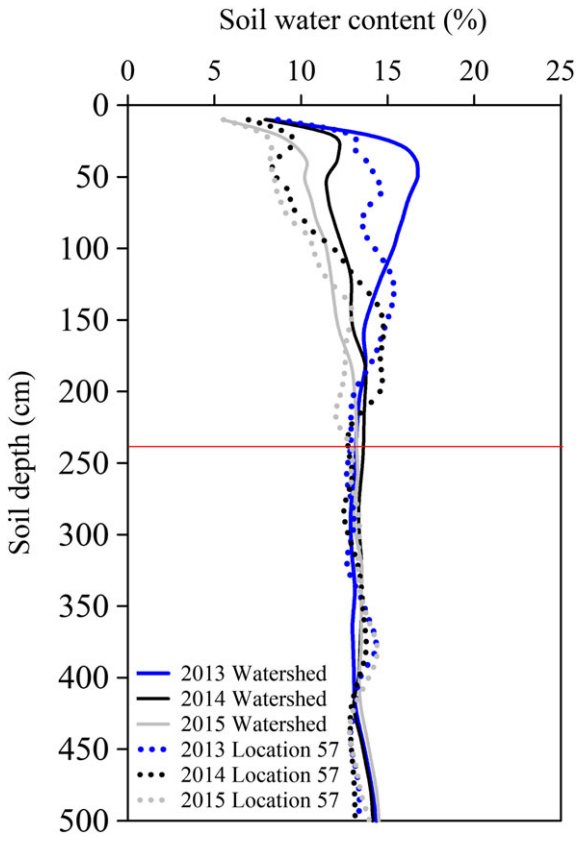

FIGURE 8 Vertical distribution of mean soil water content (SWC) in the 5-m profile measured at Location 57 and the mean SWC for LaoYeManQu watershed on the Chinese Loess Plateau from 2013 to 2015. The blue, black, and grey solid and dotted lines represent the mean SWC measured at Location 57 and mean SWC at the watershed scale in 2013, 2014, and 2015, respectively

4 | CONCLUSIONS

We measured SWC and corresponding soil properties in 5-m profiles at 73 locations for 3 years (totally, 19 times) at the LYMQ watershed. The temporal and spatial variability of SWS was greatly dependent on soil depth. The annual mean SWS decreased with depth (0–1.5 m) and was highly associated with precipitation. The changes in SWS at 1.5–5.0 m depths indicated a lag between precipitation and the replenishment of soil moisture. The geostatistical parameters of SWS were also highly depth-dependency, and the mean SWS presented similar spatial structures in contiguous soil layers. The MRD, SDRD, and MABE showed that the TS in the soil profile was significantly weaker at the surface than in deeper layers. The SWS in different layers were controlled mainly by clay, silt, sand, and organic carbon content at the watershed scale. The semivariograms of SWS, SDRD, and MABE were best fitted by an isotropic spherical model, and their spatial distributions were depth-dependent. SWC kept unchanged at deeper layers (>2.4 m) over 3 years. Because the watershed is a basic unit for the comprehensive treatment of ecological restoration on the CLP, our results are helpful for the conservation and management of soil and water resources on the CLP and possibly for other similar regions around the world.

ACKNOWLEDGMENTS

This research was supported by the National Natural Science Foundation of China (41571130083, 41530854, 41471189), the Coordination Innovation Project on Shaanxi Province Science and Technology (2015KTZDNY01-04), and the Youth Innovation Promotion Association CAS. Special thanks also go to Dr. William Black hall for his generous help in improving the manuscript.

ORCID

Yunqiang Wang http://orcid.org/0000-0003-3380-549X
Wei Hu http://orcid.org/0000-0002-5911-178X

REFERENCES

Albergel, C., Rudiger, C., Pellarin, T., Calvet, J. C., Fritz, N., Froissard, F., … Martin, E. (2008). From near-surface to root-zone soil moisture using an exponential filter: An assessment of the method based on in-situ observations and model simulations. *Hydrology and Earth System Sciences*, *12*, 1323–1337.

Brocca, L., Melone, F., Moramarco, T., & Morbidelli, R. (2009). Soil moisture temporal stability over experimental areas in Central Italy. *Geoderma*, *148*, 364–374. https://doi.org/10.1016/j.geoderma. 2008.11.004

Chaney, N. W., Roundy, J. K., Herrera-Estrada, J. E., & Wood, E. F. (2015). High-resolution modeling of the spatial heterogeneity of soil moisture: Applications in network design. *Water Resources Research*, *51*, 619–638. https://doi.org/10.1002/2013WR014964

Chen, H. S., Shao, M. A., & Li, Y. Y. (2008). The characteristics of soil water cycle and water balance on steep grassland under natural and simulated rainfall conditions in the Loess Plateau of China. *Journal of Hydrology*, *360*, 242–251. https://doi.org/10.1016/j.jhydrol. 2008.07.037

Chen, Y. P., Wang, K. B., Lin, Y. S., Shi, W. Y., Song, Y., & He, X. H. (2015). Balancing green and grain trade. *Nature Geoscience*, *8*, 739–741. https://doi.org/10.1038/ngeo2544

Coleman, M. L., & Niemann, J. D. (2013). Controls on topographic dependence and temporal instability in catchment-scale soil moisture patterns. *Water Resources Research*, *49*, 1625–1642. https://doi.org/10.1002/wrcr. 20159

Corradini, C. (2014). Soil moisture in the development of hydrological processes and its determination at different spatial scales. *Journal of Hydrology*, *516*, 1–5. https://doi.org/10.1016/j.jhydrol. 2014.02.051

Dobriyal, P., Qureshi, A., Badola, R., & Hussain, S. A. (2012). A review of the methods available for estimating soil moisture and its implications for water resource management. *Journal of Hydrology*, *458*, 110–117. https://doi.org/10.1016/j.jhydrol. 2012.06.021

Fatichi, S., Katul, G. G., Ivanov, V. Y., Pappas, C., Paschalis, A., Consolo, A., … Burlando, P. (2015). Abiotic and biotic controls of soil moisture spatiotemporal variability and the occurrence of hysteresis. *Water Resources Research*, *51*, 3505–3524. https://doi.org/10.1002/2014WR016102

Feng, Q., Liu, Y. S., & Mikami, M. (2004). Geostatistical analysis of soil moisture variability in grassland. *Journal of Arid Environments*, *58*, 357–372. https://doi.org/10.1016/j.jaridenv. 2003.08.002

Fu, B. J., Wang, J., Chen, L. D., & Qiu, Y. (2003). The effects of land use on soil moisture variation in the Danangou catchment of the Loess Plateau, China. *Catena*, *54*, 197–213. https://doi.org/10.1016/S0341-8162 (03)00065-1

Gannon, J. P., Bailey, S. W., & McGuire, K. J. (2014). Organizing groundwater regimes and response thresholds by soils: A framework for understanding runoff generation in a headwater catchment. *Water Resources Research*, *50*, 8403–8419. https://doi.org/10.1002/2014WR015498

Gao, L., & Shao, M. A. (2012). Temporal stability of shallow soil water content for three adjacent transects on a hillslope. *Agricultural*

Water Management, *110*, 41–54. https://doi.org/10.1016/j.agwat.2012.03.012

Gao, L., Shao, M. A., Peng, X. H., & She, D. L. (2015). Spatio-temporal variability and temporal stability of water contents distributed within soil profiles at a hillslope scale. *Catena*, *132*, 29–36. https://doi.org/10.1016/j.catena. 2015.03.022

Gao, X. D., Wu, P. T., Zhao, X. N., Shi, Y., & Wang, J. (2011). Estimating spatial mean soil water contents of sloping jujube orchards using temporal stability. *Agricultural Water Management*, *102*, 66–73. https:/doi.org/10.1016/j.agwat.2011.10.007

Gao, X., Zhao, X., Wu, P., Brocca, L., & Zhang, B. (2016). Effects of large gullies on catchment-scale soil moisture spatial behaviors: A case study on the Loess Plateau of China. *Geoderma*, *261*, 1–10.

Gomez-Plaza, A., Alvarez-Rogel, J., Albaladejo, J., & Castillo, V. M. (2000). Spatial patterns and temporal stability of soil moisture across a range of scales in a semi-arid environment. *Hydrological Process*, *14*, 1261–1277. https://doi.org/10.1002/(SICI)1099-1085(200005)14:7<1261::AID-HYP40>3.0.CO;2-D

Gomez-Plaza, A., Martinez-Mena, M., Albaladejo, J., & Castillo, V. M. (2001). Factors regulating spatial distribution of soil water content in small semiarid catchments. *Journal of Hydrology*, *253*, 211–226. https://doi.org/10.1016/S0022-1694 (01)00483-8

Grayson, R. B., Bloschl, G., Western, A. W., & McMahon, T. A. (2002). Advances in the use of observed spatial patterns of catchment hydrological response. *Advances in Water Resources*, *25*, 1313–1334. DOI: Pii S0309–1708 (02)00060-X

Green, T. R., & Erskine, R. H. (2011). Measurement and inference of profile soil-water dynamics at different hillslope positions in a semiarid agricultural watershed. *Water Resources Research*, *47*. https://doi.org/10.1029/2010wr010074

Hu, W., Shao, M. A., Han, F. P., Reichardt, K., & Tan, J. (2010). Watershed scale temporal stability of soil water content. *Geoderma*, *158*, 181–198. https://doi.org/10.1016/j.geoderma. 2010.04.030

Hu, W., Shao, M. A., & Reichardt, K. (2010). Using a new criterion to identify sites for mean soil water storage evaluation. *Soil Science Society of America Journal*, *74*, 762–773. https://doi.org/10.2136/sssaj2009.0235

Huang, T., Pang, Z., & Edmunds, W. M. (2013). Soil profile evolution following land-use change: Implications for groundwater quantity and quality. *Hydrological Processes*, *27*, 1238–1252. https://doi.org/10.1002/hyp.9302

Huang, T. M., & Pang, Z. H. (2011). Estimating groundwater recharge following land-use change using chloride mass balance of soil profiles: A case study at Guyuan and Xifeng in the Loess Plateau of China. *Hydrogeology Journal*, *19*, 177–186. https://doi.org/10.1007/s10040-010-0643-8

Jacobs, J. M., Mohanty, B. P., Hsu, E. C., & Miller, D. (2004). SMEX02: Field scale variability, time stability and similarity of soil moisture. *Remote Sensing of Environment*, *92*, 436–446. https://doi.org/10.1016/j.rse.2004.02.017

Jia, X., Shao, M. A., Wei, X., & Wang, Y. Q. (2013). Hillslope scale temporal stability of soil water storage in diverse soil layers. *Journal of Hydrology*, *498*, 254–264.

Jipp, P. H., Nepstad, D. C., Cassel, D. K., & De Carvalho, C. R. (1998). Deep soil moisture storage and transpiration in forests and pastures of seasonally-dry amazonia. *Climatic Change*, *39*, 395–412. https://doi.org/10.1023/A:1005308930871

Lin, H. (2006). Temporal stability of soil moisture spatial pattern and subsurface preferential flow pathways in the shale hills catchment. *Vadose Zone Journal*, *5*, 317–340. https://doi.org/10.2136/vzj2005.0058

Liu, B. X., & Shao, M. A. (2014). Estimation of soil water storage using temporal stability in four land uses over 10 years on the Loess Plateau, China. *Journal of Hydrology*, *517*, 974–984. https://doi.org/10.1016/j.jhydrol. 2014.06.003

Liu, W. Z., Zhang, X. C., Dang, T. H., Zhu, O. Y., Li, Z., Wang, J., … Gao, C. Q. (2010). Soil water dynamics and deep soil recharge in a record wet year in the southern Loess Plateau of China. *Agricultural Water Management*, *97*, 1133–1138. https://doi.org/10.1016/j.agwat.2010.01.001

Lv, L. G., Liao, K. H., Lai, X. M., Zhu, Q., & Zhou, S. L. (2016). Hillslope soil moisture temporal stability under two contrasting land use types during different time periods. *Environmental Earth Sciences*, *75*, 1. https://doi.org/10.1007/s12665–015–5238-1

Markewitz, D., Devine, S., Davidson, E. A., Brando, P., & Nepstad, D. C. (2010). Soil moisture depletion under simulated drought in the Amazon: Impacts on deep root uptake. *The New Phytologist*, *187*, 592–607. https://doi.org/10.1111/j.1469-8137.2010.03391.x

Martinez-Fernandez, J., & Ceballos, A. (2003). Temporal stability of soil moisture in a large-field experiment in Spain. *Soil Science Society of America Journal*, *67*, 1647–1656.

Mohanty, B. P., & Skaggs, T. H. (2001). Spatio-temporal evolution and time-stable characteristics of soil moisture within remote sensing footprints with varying soil, slope, and vegetation. *Advances in Water Resources*, *24*, 1051–1067.

Mu, X. M., Zhang, L., McVicar, T. R., Chille, B. S., & Gau, P. (2007). Analysis of the impact of conservation measures on stream flow regime in catchments of the Loess Plateau, China. *Hydrological Processes*, *21*, 2124–2134. https://doi.org/10.1002/hyp. 6391

Nelson, D. W., & Sommers, L. E. (1975). Determination of total nitrogen in natural-waters. *Journal of Environmental Quality*, *4*, 465–468. https://doi.org/10.2134/jeq1975.00472425000400040009x

Nielsen, D. R., & Wendroth, O. (2003). *Spatial and temporal statistics: Sampling field soils and their vegetation*. Catena Verlag.

Nyberg, L. (1996). Spatial variability of soil water content in the covered catchment at Gardsjon, Sweden. *Hydrological Processes*, *10*, 89–103.

Pachepsky, Y. A., Guber, A. K., & Jacques, D. (2005). Temporal persistence in vertical distributions of soil moisture contents. *Soil Science Society of America Journal*, *69*, 347–352.

Regalado, C. M., & Ritter, A. (2006). Geostatistical tools for characterizing the spatial variability of soil water repellency parameters in a laurel forest watershed. *Soil Science Society of America Journal*, *70*, 1071–1081. https://doi.org/10.2136/sssaj2005.0177

Rowland, L., da Costa, A. C. L., Galbraith, D. R., Oliveira, R. S., Binks, O. J., Oliveira, A. A. R., … Meir, P. (2015). Death from drought in tropical forests is triggered by hydraulics not carbon starvation. *Nature*, *528*, 119–123. https://doi.org/10.1038/nature15539

Sarris, D., Christodoulakis, D., & Korner, C. (2007). Recent decline in precipitation and tree growth in the eastern Mediterranean. *Global Change Biology*, *13*, 1187–1200. https://doi.org/10.1111/j.1365-2486.2007.01348.x

Smith, M. W., Bracken, L. J., & Cox, N. J. (2010). Toward a dynamic representation of hydrological connectivity at the hillslope scale in semiarid areas. *Water Resources Research*, *46*, W12540. https://doi.org/10.1029/2009WR008496

Steelman, C. M., Endres, A. L., & Jones, J. P. (2012). High-resolution ground-penetrating radar monitoring of soil moisture dynamics: Field results, interpretation, and comparison with unsaturated flow model. *Water Resources Research*, *48*. Artn W09538. https://doi.org/10.1029/2011wr011414

Sun, W. Y., Song, X. Y., Mu, X. M., Gao, P., Wang, F., & Zhao, G. J. (2015). Spatiotemporal vegetation cover variations associated with climate change and ecological restoration in the Loess Plateau. *Agricultural and Forest Meteorology*, *209*, 87–99. https://doi.org/10.1016/j.agrformet. 2015.05.002

Sur, C., Jung, Y., & Choi, M. (2013). Temporal stability and variability of field scale soil moisture on mountainous hillslopes in Northeast Asia. *Geoderma*, *207*, 234–243. https://doi.org/10.1016/j.geoderma.2013.05.007

Tague, C., Band, L., Kenworthy, S., & Tenebaum, D. (2010). Plot- and watershed-scale soil moisture variability in a humid Piedmont

watershed. *Water Resources Research*, *46*, Artn W12541. https://doi.org/10.1029/2009wr008078

Vachaud, G., Passerat De Silans, A., Balabanis, P., & Vauclin, M. (1985). Temporal stability of spatially measured soil water probability density function1. *Soil Science Society of America Journal*, *49*, 822–828. https://doi.org/10.2136/sssaj1985.03615995004900040006x

Vanderlinden, K., Vereecken, H., Hardelauf, H., Herbst, M., Martinez, G., Cosh, M. H., & Pachepsky, Y. A. (2012). Temporal stability of soil water contents: A review of data and analyses. *Vadose Zone Journal*, *11*. https://doi.org/10.2136/vzj2011.0178

Volpe, V., Marani, M., Albertson, J. D., & Katul, G. (2013). Root controls on water redistribution and carbon uptake in the soil–plant system under current and future climate. *Advances in Water Resources*, *60*, 110–120. https://doi.org/10.1016/j.advwatres.2013.07.008

Wang, B., Wang, Y., & Wang, L. (2017). The effects of erosional topography on soil properties in a Pinus massoniana forest in southern China. *Journal of Soil and Water Conservation*, *72*, 36–44.

Wang, D. B. (2012). Evaluating interannual water storage changes at watersheds in Illinois based on long-term soil moisture and groundwater level data. *Water Resources Research*, *48*, Artn W03502. https://doi.org/10.1029/2011wr010759

Wang, S., Fu, B., Piao, S., Lu, Y., Ciais, P., Feng, X., & Wang, Y. (2016). Reduced sediment transport in the Yellow River due to anthropogenic changes. *Nature Geoscience*, *9*, 38–41. https://doi.org/10.1038/ngeo2602

Wang, Y., Shao, M. A., & Liu, Z. (2013). Vertical distribution and influencing factors of soil water content within 21-m profile on the Chinese Loess Plateau. *Geoderma*, *193*, 300–310.

Wang, Y. Q., Hu, W., Zhu, Y. J., Shao, M. A., Xiao, S., & Zhang, C. C. (2015). Vertical distribution and temporal stability of soil water in 21-m profiles under different land uses on the Loess Plateau in China. *Journal of Hydrology*, *527*, 543–554. https://doi.org/10.1016/j.jhydrol. 2015.05.010

Wang, Y. Q., Shao, M. A., Zhu, Y. J., & Liu, Z. P. (2011). Impacts of land use and plant characteristics on dried soil layers in different climatic regions on the Loess Plateau of China. *Agricultural and Forest Meteorology*, *151*, 437–448. https://doi.org/10.1016/j.agrformet. 2010.11.016

Zhao, Y., Peth, S., Wang, X. Y., Lin, H., & Horn, R. (2010). Controls of surface soil moisture spatial patterns and their temporal stability in a semi-arid steppe. *Hydrological Processes*, *24*, 2507–2519. https://doi.org/10.1002/hyp. 7665

Zhu, Q., Nie, X. F., Zhou, X. B., Liao, K. H., & Li, H. P. (2014). Soil moisture response to rainfall at different topographic positions along a mixed land-use hillslope. *Catena*, *119*, 61–70.

How to cite this article: Fu Z, Wang Y, An Z, et al. Spatial and temporal variability of 0- to 5-m soil–water storage at the watershed scale. *Hydrological Processes*. 2018;32:2557–2569. https://doi.org/10.1002/hyp.13172